The Journal of Immunology

Immune Surveillance Properties of Human NK Cell-Derived Exosomes

Luana Lugini, Serena Cecchetti, Veronica Huber, Francesca Luciani, Gianfranco Macchia, Francesca Spadaro, Luisa Paris, Laura Abalsamo, Marisa Colone, Agnese Molinari, Franca Podo, Licia Rivoltini, Carlo Ramoni and Stefano Fais

J Immunol 2012; 189:2833-2842; Prepublished online 17 August 2012;
doi: 10.4049/jimmunol.1101988
http://www.jimmunol.org/content/189/6/2833

The Journal of Immunology is published twice each month by
The American Association of Immunologists, Inc.,
1451 Rockville Pike, Suite 650, Rockville, MD 20852

Print ISSN: 0022-1767 Online ISSN: 1550-6606.

Immune Surveillance Properties of Human NK Cell-Derived Exosomes

Luana Lugini,*[,1] Serena Cecchetti,[†,1] Veronica Huber,[‡] Francesca Luciani,[§] Gianfranco Macchia,[†] Francesca Spadaro,[†] Luisa Paris,[†] Laura Abalsamo,[†] Marisa Colone,[¶] Agnese Molinari,[¶] Franca Podo,[†] Licia Rivoltini,[‡] Carlo Ramoni,[†] and Stefano Fais*

Exosomes are nanovesicles released by normal and tumor cells, which are detectable in cell culture supernatant and human biological fluids, such as plasma. Functions of exosomes released by "normal" cells are not well understood. In fact, several studies have been carried out on exosomes derived from hematopoietic cells, but very little is known about NK cell exosomes, despite the importance of these cells in innate and adaptive immunity. In this paper, we report that resting and activated NK cells, freshly isolated from blood of healthy donors, release exosomes expressing typical protein markers of NK cells and containing killer proteins (i.e., Fas ligand and perforin molecules). These nanovesicles display cytotoxic activity against several tumor cell lines and activated, but not resting, immune cells. We also show that NK-derived exosomes undergo uptake by tumor target cells but not by resting PBMC. Exosomes purified from plasma of healthy donors express NK cell markers, including $CD56^+$ and perforin, and exert cytotoxic activity against different human tumor target cells and activated immune cells as well. The results of this study propose an important role of NK cell-derived exosomes in immune surveillance and homeostasis. Moreover, this study supports the use of exosomes as an almost perfect example of biomimetic nanovesicles possibly useful in future therapeutic approaches against various diseases, including tumors. ***The Journal of Immunology*****, 2012, 189: 2833–2842.**

Secretory lysosomes are highly differentiated organelles with a dual function. In fact, they combine catabolic functions of conventional lysosomes with an inducible secretory potential, exerting a key role in the homeostatic cross-talk between hematopoietic cells (1). Like conventional lysosomes, these secretory vesicles are acidic and contain common hydrolases and membrane proteins; differently from typical lysosomes, they undergo a regulated secretion and fusion with the plasma membrane (2). In fact, it has been shown that the lytic granules of CTLs and NK cells are secretory lysosomes, expressing typical lysosomal markers and containing perforin and granzymes (3, 4). Moreover, it has been demonstrated that newly synthesized Fas ligand (FasL) is stored in specialized secretory lysosomes in both CTLs and NK cells and that polarized degranulation controls the delivery of FasL to the cell surface (5). This finding was consistent with both the involvement of a FasL-dependent pathway in CTL and NK cell-mediated cytotoxicity (5) and the demonstration that the ligands for death receptors released by CTLs into the immunological synapse are not in a soluble form but rather membrane enveloped (6). Lately, a heterogeneous family of secreted organelles, called exosomes, is acquiring a growing importance in the regulation of several normal cellular functions but also in the development of human diseases, including cancer, neurologic, infectious, and autoimmune diseases (7–9). Exosomes are nanovesicles (50–100 nm diameter) released by a great variety of cells, including normal cells of either hematopoietic or epithelial origin, but also tumor- and virus-infected cells (10, 11). The major hypothesis on their cellular origin involves a process of endosome-to-lysosome-to-phagosome fusion that often includes the plasma membrane, with the final formation of ad hoc structures called multivesicular bodies (10). Exosomes have been shown to be involved in a variety of functions related to their cellular source, including immune stimulation or suppression, cell-to-cell communication, delivery of proteins and genetic material, cell-free viral infection, tumor immune escape, and tumor cell communication (10–17). One example of the bioactivity of exosomes is their capacity to trigger cell death through ligands for death receptors, such as FasL carried by these nanovesicles (2, 18). This was demonstrated for exosomes released by activated human T cells (19) and tumor cells of different histotypes, including melanoma (18) and colon carcinoma (20). In tumor patients, the level of circulating exosomes is 3- to 4-fold higher than in healthy individuals and correlates with the degree of malignancy (21).

Exosomes of normal human cells, such as B, T, and epithelial cells, have been widely characterized, especially those derived from dendritic cells, also called dexosomes (22, 23). Dendritic cell-derived exosomes have also found their way into the clinic; in fact, they have been used as antitumor therapy in patients affected by

*Department of Therapeutic Research and Medicines Evaluation, National Institute of Health, 00161 Rome, Italy; [†]Department of Cell Biology and Neurosciences, National Institute of Health, 00161 Rome, Italy; [‡]Unit of Immunotherapy of Human Tumors, Foundation of Institutes for Treatment and Research, National Cancer Institute, 20133 Milan, Italy; [§]Center for Immunobiologicals Research and Evaluation, National Institute of Health, 00161 Rome, Italy; and [¶]Department of Technologies and Health, National Institute of Health, 00161 Rome, Italy

[1]L.L. and S.C. contributed equally to this work.

Received for publication July 8, 2011. Accepted for publication July 8, 2012.

This work was supported by a Special Research Program in Oncology, Italian Ministry of Heath Grant Onc_Ord 37/07 ISS N° 70CF/4 (to S.F.).

Address correspondence to Dr. Stefano Fais, Department of Therapeutic Research and Medicines Evaluation, National Institute of Health, Viale Regina Elena, 299, 00161 Rome, Italy. E-mail address: stefano.fais@iss.it

The online version of this article contains supplemental material.

Abbreviations used in this article: CLSM, confocal laser scanning microscopy; FasL, Fas ligand; IP, immunoprecipitation; LAK, activated NK cell; LAKEXO, LAK-derived exosome; mFasL, membrane FasL; MHC-I, MHC class I; NCR, natural cytotoxicity receptor; NKEXO, NK-derived exosome; PI, propidium iodide; sFasL, soluble FasL.

www.jimmunol.org/cgi/doi/10.4049/jimmunol.1101988

different tumor histotypes in clinical trials, albeit with poorly encouraging results. However, among the exosomes released by "normal" cells, those secreted by NK cells have been widely neglected.

In view of the important role of NK cells as innate immunity members in tumor immune surveillance, we investigated NK exosomes as surrogates of this cell population sharing the ability of recirculating in body fluids. In this paper, we show that human NK cells release exosomes in both resting and activated condition. These small vesicles express both typical NK markers (i.e., CD56) and killer proteins (i.e., FasL and perforin) and display antitumor and immune homeostatic activities. The in vitro data presented in this paper were strongly supported by ex vivo findings on plasma-derived exosomes of healthy donors, showing expression of NK markers, such as CD56 and perforin, and exosome-induced cytotoxicity. Thus, it appears conceivable that NK-derived exosomes may have a role in both paracrine and systemic control of the immune response.

To our knowledge, this is the first report on phenotypical and functional properties of exosomes derived from human NK cells, thus adding new data in this poorly explored field.

Materials and Methods

Cell cultures

Buffy coats of 11 healthy donors were provided by Centro Trasfusionale Universitario Azienda Policlinico Umberto I in Rome, Italy (the study was approved by the ethical committee of Istituto Superiore di Sanità, Rome, Italy, and donors gave written-informed consent to participate). Human PBMC were then isolated from buffy coats by Ficoll-Histopaque 1077 gradient (Sigma-Aldrich, St. Louis, MO). Resting NK cells were further purified by negative immunomagnetic selection, using a specific combination of anti-CD3, anti-CD4, anti-CD8, anti-CD20, and anti-CD14 mAbs (OKT3, OKT4, OKT8, OKT20, and 63D3), produced in-house from culture supernatants of corresponding hybridoma (American Type Cell Culture). Cells were then incubated with magnetic beads coated with goat anti-mouse IgG (Dynal, Oslo, Norway). The resulting NK cell population was >90% $CD56^+$, $CD3^-$, and $CD14^-$, as assessed by cytofluorimetric analyses (cell viability ≥ 99%). Next, purified resting NK cells were cultured for 3 d at the high density of 5×10^6/ml to reduce cell death (cell viability ≥ 90%).

Activated NK cells (LAK cells) were obtained by coculturing PBMC from buffy coats (4×10^5 cells/ml) with cobalt-irradiated (4000 rad) RPMI 8866 cells (B lymphoblastoid cell line) (1×10^5 cells/ml) at 37°C in a humidified 7% CO_2 atmosphere for 10 d, as described previously (24). On day 7, the contaminating T cells were eliminated by indirect negative immunomagnetic depletion by mixed anti-CD3, anti-CD4, and anti-CD8 mAbs (as described above for resting NK cells), and the resulting cell population was >95% pure, as assessed by flow cytometry analyses. Then, the purified NK cells subset was incubated with human rIL-2 (100 U/ml; Hoffman-La Roche, Nutley, NJ) for 3 d (cell viability ≥ 90%). Using this culture method, an average of 25-fold increase in activated NK cell number was obtained.

The following human tumor cell lines were used: Jurkat (T cell leukemia), K562 (erythroleukemia), DAUDI (Burkitt lymphoma) (all obtained from American Type Cell Culture), SKBR3 (metastatic breast adenocarcinoma) (a gift from Dr. P. Natali, Istituto Tumori Regina Elena, Rome, Italy), and 501mel (metastatic melanoma cell line) (25). The activation of PBMC was performed by incubating cells with 1 μg/ml PHA (Murex Biotech, Dartford, U.K.).

All tumor cell lines, PBMC and NK and LAK cells, were cultured in RPMI 1640 medium (Life Technologies, Grand Island, NY), supplemented with 10% exosome-depleted FBS, 100 U/ml penicillin, 100 μg/ml streptomycin (Life Technologies), and 2 mmol/l glutamine in a 5% CO_2 environment at 37°C.

All cell lines were negative for mycoplasma contamination, as routinely tested by a PCR Mycoplasma detection kit (Venor GeM; Minerva Biolabs, Berlin, Germany).

Isolation of exosomes

Human resting NK cells and LAK cells were cultured as described above. The culture supernatants were subjected to differential centrifugation as previously described in standard protocol exosomes preparation (26) Briefly, cell culture medium was centrifuged for 5 min at 300 × *g*, 20 min at 1,200 × *g*, and 30 min at 10,000 × *g* to remove cells and debris. Membrane vesicles were collected by ultracentrifugation at 100,000 × *g* for 60 min at 19°C using a Beckman TL 100.2 rotor (Beckman Instruments, Fullerton, CA). The resulting pellet was washed in a large volume of PBS and again ultracentrifuged at 100,000 × *g* for 60 min. Exosomes were resuspended in PBS or RPMI 1640 medium or dissolved in lysis buffer for further analyses.

To obtain healthy donor plasma-derived exosomes, we followed a previously modified protocol (27), in which after the separation from total blood, previously diluted 1:1 with HBSS, plasma was centrifuged for 30 min at 500 × *g*, 45 min at 12,000 × *g*, and 2 h at 110,000 × *g* at 19°C using a Beckman TL 100.2 rotor. The resulting pellet was washed in PBS, filtered through a 0.22-μm filter (Millipore, Billerica, MA), ultracentrifuged at 110,000 × *g* for 1 h, and resuspended in PBS, RPMI 1640 medium, or lysis buffer, depending on further analyses.

Immunoelectron microscopy

Immunoelectron microscopic analysis was performed on isolated NK exosomes as follows.

A drop of exosome suspension was placed onto a formvar–carbon-coated grid. The exosomes put down on the grids were washed twice with PBS, incubated with rabbit polyclonal anti-Rab5B (A-20; Santa Cruz Biotechnology, Heidelberg, Germany) or mouse monoclonal anti-CD56 (123C3; Santa Cruz Biotechnology) for 1 h at room temperature, washed twice in PBS, and labeled with anti-rabbit IgG or anti-mouse IgG 5-nm-diameter-gold particle-conjugated Ab (Sigma-Aldrich) for 45 min at room temperature. After three washes in Aurion BSA-c solution, two washes in PBS, and a final wash in distilled water, grids were negative stained with uranyl acetate solution. Samples were examined with a Philips 208 transmission electron microscope (FEI Company, Eindhoven, The Netherlands). This method ensured the best antigenic preservation, allowing labeling of only the surface components.

Sucrose gradient of exosomes

Floatation of exosomes was performed on a continuous sucrose gradient, using a Beckman SW41 rotor as previously described (12), with some modifications. Briefly, exosomes were resuspended in 2 ml 2.5 M sucrose and 20 mM HEPES/NaOH (pH 7.2). A linear sucrose gradient (2.0–0.25 M sucrose and 20 mM HEPES/NaOH [pH 7.2]) was layered on top of the exosomes suspension in a SW41 tube, and the sample was centrifuged at 100,000 × *g* for 16 h at 4°C. Gradient fractions (12 × 1 ml) were collected from the top of the tube, diluted with 1.0 ml PBS, and ultracentrifuged at 100,000 × g for 1 h in a Beckman TL 100.2 rotor. Fractions density was evaluated using an Abbé Refractometer (Carl Zeiss, Oberkochen, Germany). Exosomes in each fraction were then lysed and processed by SDS-PAGE and Western blotting.

Immunoprecipitation and Western blotting

Purified exosomes or cells were lysed in lysis buffer (1% Triton X-100, 0.1% SDS, and 0.1 M Tris-HCl [pH 7]) and protease inhibitors (Hoffman-La Roche). Protein content was measured by Bradford assay (Bio-Rad, Hercules, CA), according to the manufacturer's instructions, solubilized in Laemmli loading buffer, and analyzed under reducing conditions by SDS-PAGE, followed by electroblotting on nitrocellulose membranes (Protran Whatman, Dassel, Germany). Membranes were incubated with following primary Abs: rabbit anti-Rab5B (A-20; Santa Cruz Biotechnology), goat anti-calregulin (T-19; Santa Cruz Biotechnology), mouse anti-prohibitin (II-14-10; Novus Biologicals, Cambridge, U.K.), mouse anti-nucleoporin p62 (BD Biosciences, Heidelberg, Germany), mouse anti-MHC class I (MHC-I) (anti-human HLA-A/B/C; DakoCytomation, Milan, Italy), mouse anti-Golgi 58K (58K-9; Sigma-Aldrich), mouse anti-FasL (G247-4; BD Pharmingen, San Diego, CA), and rabbit anti-Perforin 1 (H-315; Santa Cruz Biotechnology) and then incubated with HRP–goat (Santa Cruz Biotechnology), HRP–rabbit or HRP–mouse secondary Abs (Amersham Biosciences, Milan, Italy). Bands were detected using an ECL kit (Pierce, Rockford, IL). Immunoprecipitation (IP) experiments were performed as following: LAK cells or LAK-derived exosomes were pelleted, washed with PBS, and lysed in lysis buffer (20 mM Tris-HCl [pH 7.5], 150 mM NaCl, 10% glycerol, and 1% Nonidet P-40) and proteases inhibitors (Hoffman-La Roche). Proteins were precleared with protein A+G–Sepharose 4B Fast Flow (Sigma-Aldrich) for 1 h at 4°C. FasL molecule was immunoprecipitated from precleared lysate with mouse anti-FasL (NOK-1; BD Pharmingen) overnight at 4°C in the presence of 10% protein A+G–Sepharose. Immunoprecipitated beads were washed in AKT

buffer, resuspended in SDS sample buffer, and analyzed by Western blot as described above. For the IP experiments using DynabeadsM-280 Tosyl-activated (Invitrogen Life Technologies, Monza, Italy), we first coupled the Ab anti-FasL, in a buffer containing 0.1 M borate buffer (pH 9.5) and 3 M ammonium sulfate, to the beads by incubating them on a roller at 37°C overnight. Then, 500 μg protein lysate, both from LAK cells and LAK-derived exosomes, prepared as described above, was added to the FasL Ab-coupled Dynabeads and incubated for 4 h at room temperature with tilting and rotation to capture the target protein. FasL-captured protein was then eluted off the Dynabeads by the addition of 0.1 M glycine (pH 3) plus 0.1% Triton X-100 and 1.5 M Tris (pH 8) and then by a magnetic separation. The isolated pure protein fractions were then resuspended in SDS sample buffer and analyzed by Western blot.

Confocal microscopy analysis

For confocal laser scanning microscopy (CLSM), Jurkat cells or resting PBMC were labeled with PKH67 dye (Green Fluorescent cell linker kit; Sigma-Aldrich) as follows: the cells were incubated in diluent C plus PKH67 for 5 min, followed by quenching with FBS, and then washed with PBS. Meanwhile, LAK-derived exosomes were labeled at 1:3 (w/w) protein exosomes:NHS-Rhodamine (Pierce) for 30 min at 4°C in PBS, followed by quenching with serum-free RPMI 1640 medium, then washed in PBS by centrifugation at 100,000 × *g* for 1 h. After 5 h of coincubation between exosomes and cells and a wash in PBS, the PKH67-labeled Jurkat or PBMC were seeded on coverglass coated with poly-L-lysine (Sigma-Aldrich) for 15 min at 4°C and, after washing with PBS, were observed in vivo without fixation with a Leica TCS SP2 Acousto-Optical Beam Splitter apparatus, equipped with a HCX PL apochromatic ×63 oil immersion objective (numerical aperture lenses 1.40), using excitation spectral laser lines 488 and 543 nm for PKH67 and NHS-Rhodamine, respectively. Signals from these different fluorescent probes were taken in sequential scan mode. Image acquisition and processing were carried out using the Leica Confocal Software (Leica Mycrosystems, Wetzlar, Germany) and Adobe Photoshop software programs (Adobe Systems, San Jose, CA). Several fields were analyzed for each labeling condition, and representative results are presented.

Flow cytometry

Characterization of exosomes. Purified exosomes were incubated with 4-μm-diameter aldehyde/sulfate latex beads (Interfacial Dynamics) in PBS overnight at 4°C under gentle agitation. After washing with PBS, samples were resuspended in PBS/0.5% BSA and incubated with the following Abs: anti–CD16-PE, anti–CD56-PE, anti–CD4-PE, anti–CD8-PE, anti–NKG2D-PE (all from BD Pharmingen), anti–NKp30-PE, anti–NKp40-PE, anti–NKp44-PE (Immunotech–Beckman Coulter, Marseilles, France), anti-CD63 (MX-49.129.5), anti-Rab5B (A-20) (all from Santa Cruz Biotechnology); these later were followed by Alexa Fluor 488-conjugated secondary Abs (Molecular Probes) and analyzed using a FACSCalibur flow cytometer (BD Biosciences) and CellQuest Software (BD Biosciences). To detect FasL and perforin molecules by the Abs anti-FasL (NOK-1; BD Pharmingen) and anti-Perforin 1 (H-315; Santa Cruz Biotechnology) NK and LAK-derived exosome (LAKEXO) were permeabilized by 0.5% Triton X-100 prior to incubation with the Abs. A minimum of 5×10^3 beads/sample were examined.

Cytotoxic assay. Cytolysis was assessed, measuring the cell uptake of propidium iodide (PI) by flow cytometry analysis, as previously described with some modifications (28, 29). Briefly, purified exosomes were used as effectors and mixed with different target cells, either PBMC or tumor cell lines, at the ratios of 60 μg NK-derived exosome (NKEXO) and LAKEXO or 300 μg plasma-derived exosomes to 50×10^3 target cells in complete medium at 37°C in 5% CO_2. Cells were harvested after a 1.5-, 5-, and 24-h culture, washed in PBS, and incubated with PI (20 μg/ml; Molecular Probes) for 10 min at room temperature and rewashed in PBS. Finally, the cells were fixed in 1% paraformaldehyde and analyzed by flow cytometry. The mean fluorescence of triplicate samples was used in all cytotoxicity calculations. The maximum level of PI uptake was determined in target cells lysed by 0.5% Triton X-100. Cytotoxicity was expressed as the percentage of cell deaths among target cells: (number of dead cells/[number of dead cells + number of live cells]) × 100. The percentage of dead target cells was corrected for spontaneous background cell death by subtracting the percentage of dead cells in control samples.

Apoptosis and necrosis analysis. To evaluate simultaneously necrosis, apoptosis, and living cells, we used the PI supravital staining as described previously (30). Briefly, nonpermeabilized cells were incubated with 40 μg/ml PI for 1.5 h at 37°C and analyzed by flow cytometry. Apoptotic cells were detected on a forward light scatter/PI dot plot as a PI^{dim} peak, whereas necrotic/late apoptotic cells were detected as a PI^{bright} peak, and PI^{neg} represented live cells.

For assessing FasL/Fas involvement, Jurkat cells were preincubated for 1 h at 37°C with 100 ng/ml anti-Fas mAb (ZB4; Upstate Biotechnology, Waltham, MA) and then cocultured with NK-derived exosomes for 1.5, 5, or 24 h. Then, cells were analyzed using the PI supravital staining method, as described above.

Supplemental materials and methods

For CLSM analyses, 15 μg exosomes were incubated with 5 μl 4-μm-diameter aldehyde/sulfate latex beads (Interfacial Dynamics, Portland, OR) at room temperature in a small volume of PBS. After 15 min, the PBS volume was increased to 1.0 ml and incubated overnight at 4°C under gentle agitation. After three washings in PBS/0.5% BSA, exosome-coated beads were resuspended in PBS/0.5% BSA and then seeded on coverglass coated with poly-L-lysine (Sigma-Aldrich) for 15 min at 4°C. After washing with PBS, samples were fixed by 3% paraformaldehyde (30 min, 4°C), permeabilized by 0.5% Triton X-100 (10 min at room temperature), and stained (30 min, 37°C) with FasL (NOK-1) (BD Pharmingen) or Perforin 1 (H-315) (Santa Cruz Biotechnology) Abs for the detection of intracellular proteins. Conversely, to detect membrane molecules, exosome-coated beads were directly stained, without permeabilization, with the following primary Abs (30 min, 4°C): Rab5B (A-20) and CD63 (MX-49.129.5) purchased from Santa Cruz Biotechnology; CD56, CD4, and CD8 (BD Pharmingen); and followed by Alexa Fluor 488-conjugated secondary Ab (Molecular Probes, Eugene, OR). The glass was then mounted

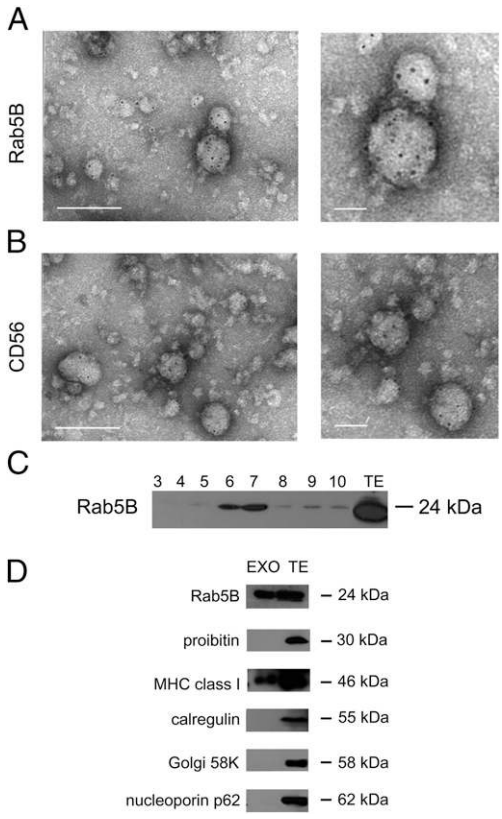

FIGURE 1. Morphological and biochemical characterization of NK-derived exosomes. Immunoelectron microscopy of isolated NK–exosomes incubated with anti-Rab5B (**A**) or anti-CD56 (**B**), followed by IgG 5-nm-diameter-gold particle-conjugated Ab. In the *right panels*, magnified images are reported. Scale bars, 100 nm (*left panels*) and 50 nm (*right panels*). Representative of three independent experiments are reported. (**C**) Western blot analysis of sucrose gradient fractions of exosomes isolated from resting NK cell culture supernatant. The density in which exosomes float corresponds to the Rab5B-positive fractions, and it is comprised between 1.10 and 1.19 g ml^{-1} (six and seven fractions). TE, total cell protein extract. (**D**) Western blot analysis of constitutive exosome markers (i.e., Rab5B and MHC-I) compared with cell markers for endoplasmic reticulum (calregulin), Golgi (Golgi 58K), mitochondrial (prohibitin), or nucleus (nucleoporin p62) markers. EXO, exosome total protein extract.

on the microscope slide with the Vectashield Mounting Medium (Vector Laboratories, Burlingame, CA), and CLSM observations were performed with a Leica TCS SP2 Acousto-Optical Beam Splitter apparatus, equipped with an HCX PL apochromatic ×63 oil immersion objective (numerical aperture lenses 1 × 40), using a 488-nm excitation spectral laser line appropriately tuned by acousto-optical tunable filter. Image acquisition and processing were carried out using the Leica Confocal Software (Leica Lasertechnik, Heidelberg, Germany) and Adobe Photoshop software programs (Adobe Systems, San Jose, CA). Several fields were analyzed for each labeling condition, and representative results are presented.

Results

Characterization of human resting and activated NK cell-derived exosomes

With the purpose of evaluating the level of exosome production by either resting or activated NK cells, human resting NK cells isolated from blood of healthy donors were cultured for 3 d, and the cell culture supernatant was subjected to sequential low-speed and high-speed centrifugation, as described previously (26). Protein content analysis of the exosomal fraction revealed that resting NK cells constitutively release a large amount of exosomes (NKEXO) as measured by Bradford assay. Despite a great variability between the healthy donors (n = 11), we could detect substantial amounts of exosomal proteins released by resting NK cells in all cases (5.3 ± 3 μg/1 × 10^6 cells).

Electron microscopy was exploited to analyze our nanovesicles preparation from NK cell supernatants from both a morphological point of view and expression of markers of exosomes and NK cells. The results have shown that NK cell-derived supernatants contained vesicles that resembled exosomes in both size (40–100 nm) and vesicular morphology (Fig. 1A, 1B) (10, 12). Moreover, the immunoelectron microscopy showed a clear positivity for both a constitutive exosomal marker, Rab5B (Fig. 1A) (10, 31), and a typical NK cell marker, CD56 (Fig. 1B).

Sucrose gradient centrifugation showed NK cell-derived exosomes floating at the typical density between 1.10 and 1.19 g ml^{-1}, as shown by Western blot analysis of Rab5B protein in the gradient fractions (Fig. 1C) and in agreement with previously reported data on exosome isolated from cell culture supernatant (12).

Further characterization of NK cell exosomes by Western blot analysis confirmed the presence of typical exosomal proteins, such as Rab5B and MHC-I, but also excluded the presence of contaminating proteins from endoplasmic reticulum, Golgi, mito-

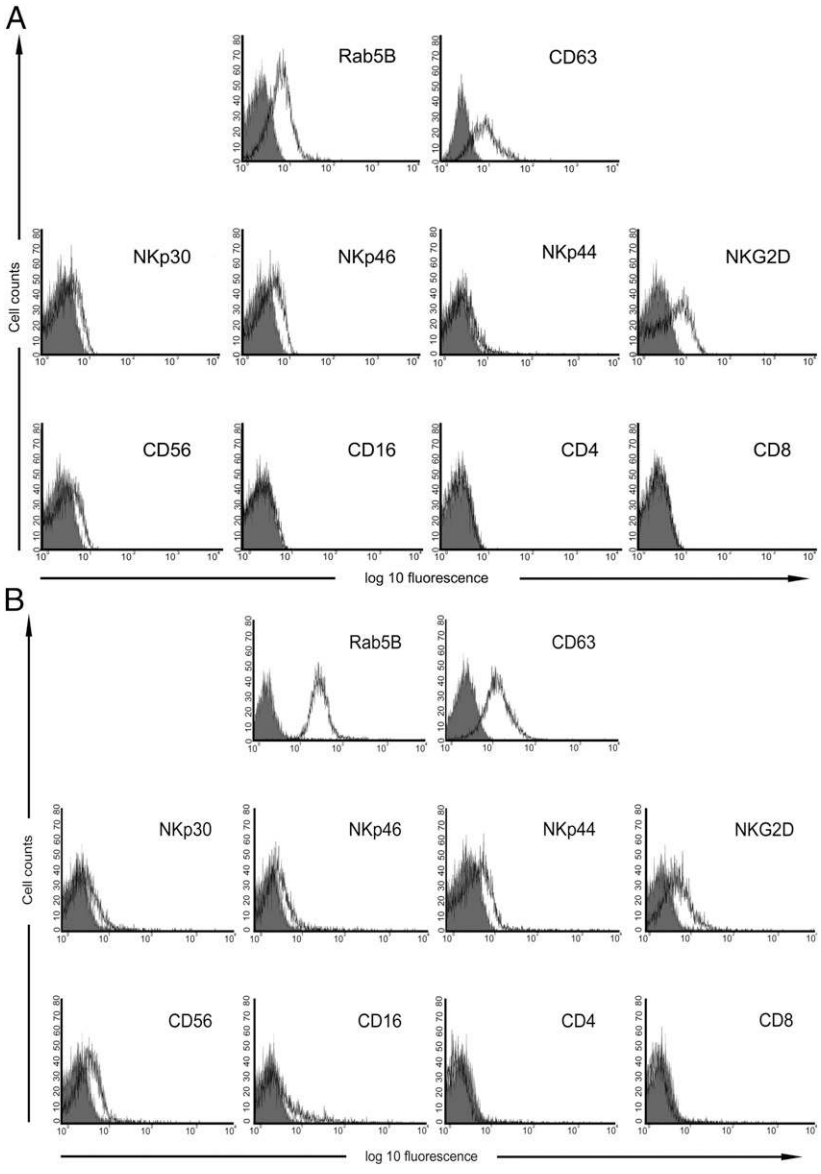

FIGURE 2. Flow cytometry analyses of NKEXO and LAKEXO. After purification, NK-derived (**A**) and LAK-derived (**B**) exosomes were complexed to latex beads (4-μm diameter) and stained with the indicated primary Abs, eventually followed by Alexa Fluor 488-conjugated secondary Abs. The histograms showed in gray correspond to the isotype controls of the respective Abs, whereas the white histograms indicate the positive fluorescence. Representative of five independent experiments were reported.

chondrial, or nucleus (i.e., calregulin, Golgi 58K, prohibitin, and nucleoporin molecules, respectively), potentially deriving from apoptotic or dead cells, as compared with NK cell lysates (Fig. 1D). These results were consistent with those obtained with flow cytometry analysis after exosomes coupling to latex beads. In fact, NKEXO expressed appreciable levels of both Rab5B, CD63, further confirming their exosomal nature, as well as NKG2D proteins and a substantial but lower amount of CD56, NKp30, NKp46, and NKp44 molecules, whereas CD16 receptor (FcγRIIIA), CD4, and CD8 were undetectable (Fig. 2A). The flow cytometric data were further supported by CLSM analysis, performed after coupling exosomes to latex beads, showing the expression of both exosome markers (i.e., Rab5B and CD63) and NK cell markers (i.e., CD56) and the absence of CD4 and CD8 in NK cell exosomes (Supplemental Fig. 1).

In the next set of experiments, we investigated potential differences in exosome release between resting and LAK cells. To this purpose, we purified exosomes from supernatant of both activated and resting NK cells, as described in *Materials and Methods*. The results showed that also activated NK cells released substantially high amounts of exosomes (LAKEXO), but with no significant quantitative differences with exosomes released by resting NK cells (NKEXO, 5.3 ± 3 μg/1 × 10^6 cells, versus LAKEXO, 5.4 ± 3 μg/1 × 10^6), suggesting that exosome release is a constitutive NK cell function, not requiring activation to be either triggered or simply increased.

To assess possible differences in surface marker expression between NKEXO and LAKEXO, flow cytometry analysis after coupling exosomes to latex beads was used. The analysis again did not show substantial differences between the two exosome populations but some scattered increase in Rab5B and CD63 expression in LAKEXO (Fig. 2B), as compared with resting NK-derived exosomes (Fig. 2A). The expression of exosome (i.e., Rab5B and CD63) and NK cell markers (CD56) in LAK cell-derived exosomes coupled to latex beads was confirmed by CLSM analysis as well (Supplemental Fig. 1).

Expression of FasL and perforin molecules in NK cells-derived exosomes

CTL and NK cells are known to exert their cytolytic activity through release of cytotoxic effectors (i.e., perforin) contained in lytic granules. Upon target cell recognition and conjugation, the granules are actively directed to the site of cell–cell contact, and soluble effector molecules are released into the forming cytotoxic immunological synapse. At the same time, several transmembrane components of the granules, such as FasL, are exposed on the cell surface and dictate the fate of effector and target cells (4).

Thus, we first evaluated the presence of FasL and perforin on both resting and activated NK exosomes by flow cytometry and CLSM analyses of exosome-bead complexes. The results showed that FasL and perforin molecules were equally expressed on both NKEXO and LAKEXO (Fig. 3A, 3B, respectively, Supplemental Fig. 2). Further analyses of resting and activated NK exosome preparations (Fig. 3C) demonstrated the presence of a membrane isoform of FasL (mFasL) but at a higher molecular mass (~50 kDa) as compared with the typical membrane FasL (40 kDa).

Moreover, Western blot analysis revealed also the presence of the soluble FasL isoform (sFasL; 26 kDa) in NK and LAK cell-derived exosome preparations, whereas total lysates of resting NK and LAK cells showed the presence of mFasL at the typical molecular mass of 40 kDa (Fig. 3C). To verify that the 50-kDa band detected in exosome lysates was actually a FasL isoform, we performed FasL IP experiments by two different IP approaches (see *Materials and Methods* for technical details). Both the IPs were blotted with an anti-FasL Ab (G247-4 clone), different from that used for IP (NOK-1 clone). In a first set of IP experiments, we immunoprecipitated with the classical Protein A+G–Sepharose protocol (Fig. 3D, *left panel*), and we mostly detected a band at 50 kDa in the exosome sample. To avoid the background given by the 50-kDa band of IgG, which could also mask the FasL isoform ~50 kDa, we performed the same IP using magnetic tosylactivated Dynabeads. As reported in Fig. 3D, *right panel*, the IP confirmed that exosomes express a FasL isoform at a higher molecular mass.

The expression of perforin was detected in both exosomes preparations and total cell lysates (Fig. 3C), being higher in these later. Notably, when exosomes were loaded on a linear sucrose gradient (Fig. 3E), perforin was detected in the same fractions as Rab5B (Fig. 1C), thus strongly supporting the presence of perforin in NK exosomes.

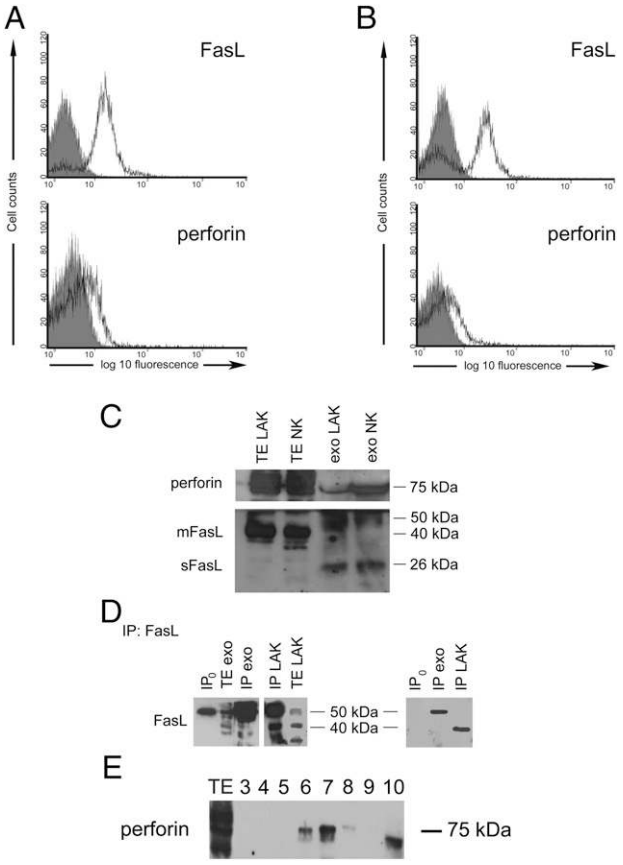

FIGURE 3. Killer proteins identification in NKEXO and LAKEXO. Flow cytometry analyses of NK-derived (**A**) or LAK-derived (**B**) exosomes loaded to latex beads and stained for FasL and perforin proteins. The histograms showed in gray correspond to the isotype controls of the respective Abs, whereas the white histograms indicate the positive fluorescence. (**C**) Western blot analysis of both LAK and NK cells total protein extracts (35γ/lane; total cell protein extract [TE] LAK and TE NK) compared with the corresponding exosome extracts (35γ/lane; exo LAK and exo NK) for the detection of perforin, mFasL, and sFasL molecules. (**D**) FasL (G247 clone) immunoblotting analyses on TEs of LAK cells (TE LAK) and LAK-derived exosomes (TE exo) and on the corresponding FasL (NOK-1 clone) IPs (IP exo and IP LAK). IP_0, appropriate control IgG. In the *left panel* is reported the result obtained by using the classical protein A+G–Sepharose approach, whereas in the *right panel* is shown the result of IP by magnetic tosylactivated Dynabeads (for technical details see *Materials and Methods*). (**E**) Western blot analysis of sucrose density gradient of exosomes isolated from resting NK cell culture supernatant, indicating the presence of perforin-positive exosomes in the fractions corresponding to 1.10 and 1.19 g ml^{-1} density (fractions 6 and 7). Data are representative of at least three experiments.

Cytolytic activity of NK cell-derived exosomes

To test the potential bioactivity of FasL and perforin expressed by NK exosomes, we investigated their cytotoxic effect against various human tumor cell lines of different histologies, including hematological malignancies (leukemia and lymphoma cells) and solid tumors (breast cancer and melanoma cells). As source of exosomes, we used LAK cells, allowing to collect high amount of exosomes in a more repeatable way. First, we evaluated the dose- and time-dependent cytotoxic effect of LAKEXO using leukemia cells (Jurkat) as target. As shown in Fig. 4A, the cytotoxic effect of LAK exosomes was time and dose dependent, reaching its highest effect at 60 μg (48.9 ± 5.2%) at 1.5 h, progressively decreasing within the next 24 h (26.8 ± 2.1% at 5 h and 9.4 ± 1.0% at 24 h). These data suggested that LAKEXO can exert a strong and quick cytotoxic activity on leukemia cells. We then tested the cytotoxic activity of 60 μg LAK exosomes on human cell lines of different tumor origin, such as leukemia (Jurkat and K562 cells), lymphoma (DAUDI cells), breast cancer (SKBR3 cells), and metastatic melanoma (501mel) (Fig. 4B). The results showed that LAKEXO induced cytotoxicity in all the tumor cell lines of hematologic origin, whereas the cell lines deriving from solid tumors (breast cancer SKBR3 and melanoma 501mel) appeared to be rather resistant to LAKEXO-mediated lysis within 24-h coculture (Fig. 4B).

Jurkat cells showed the highest sensitivity to LAKEXO-mediated lysis as soon as 1.5 h after incubation (49.9 ± 5.8% PI^+ cells). At later time points (5 and 24 h; 26.8 ± 3.4 and 11.8 ± 2.9%, respectively), the percentage of PI^+ Jurkat cells decreased continuously. In contrast, lymphoma cells (DAUDI) showed the highest cell death levels 5 h after incubation (37.1 ± 3.4%), as compared with 18.0 ± 4.8% at 1.5 h, suggesting that these cells are more resistant to lysis with respect to Jurkat cells. LAKEXO-mediated lysis of K562 leukemia cells reached a maximum of PI uptake of 20% at 1.5 h coculture, remaining constant at 5 h to then decrease at the 24-h time point (Fig. 4B).

In the previous set of experiments, we have shown that NK cells released large amounts of bioactive FasL- and perforin-positive exosomes. It appears conceivable that these exosomes may have both a role in controlling tumor growth but also in regulating the immune response. In the purpose to clarify this last hypothesis, we tested the lytic activity of activated NK exosomes on resting and PHA-activated PBMC. The results showed a significant cytotoxic activity against activated PBMC within 5 h of coincubation with LAKEXO (ranging from 20.5 ± 9.6% at 1.5 h up to 33.5 ± 4.8% at 5 h), whereas no detectable cytotoxic effect was observed against resting PBMC (Fig. 4C).

In parallel to the experiments with LAKEXO, we analyzed the effects of resting NK-derived exosomes against tumor and normal target cells. The results showed that NKEXO-induced cytotoxicity was comparable to that obtained with LAKEXO (data not shown).

This set of experiments suggested that exosomes released by both LAK and NK cells induced comparable cytolytic activity against tumor and activated immune cells, whereas resting immune

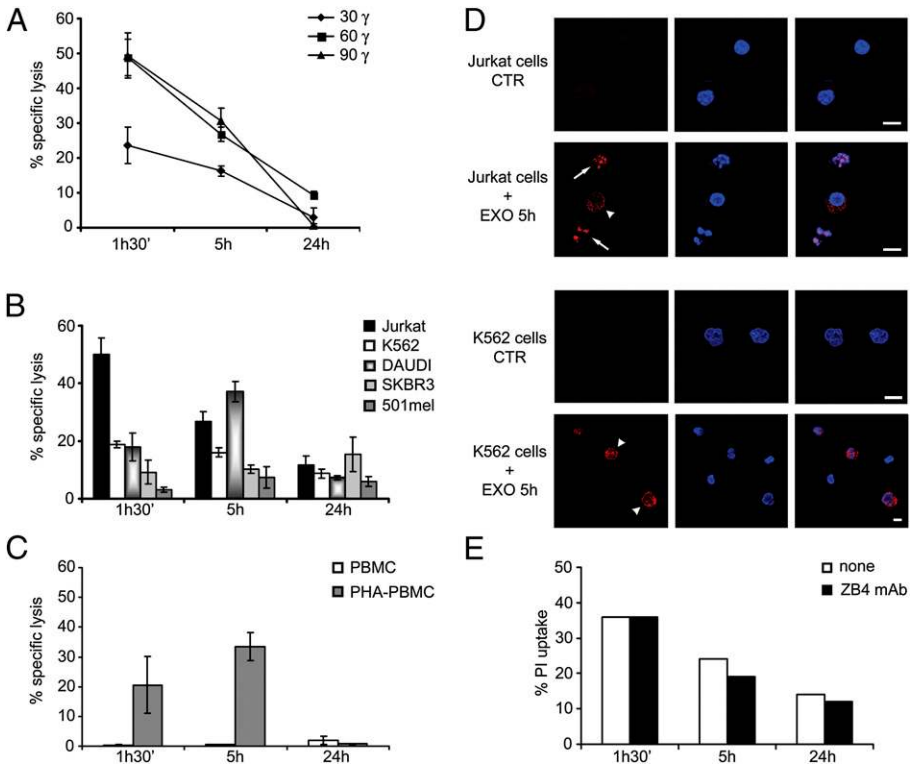

FIGURE 4. Cytolytic activity of LAKEXO. Cytotoxic activity was evaluated by flow cytometry measuring the cell uptake of PI (for details see *Materials and Methods*). (**A**) Dose-response curve of exosomes lytic activity toward Jurkat cells, used as target, at the indicated amounts (♦ 30γ, ■ 60γ, ▲ 90γ) and time points (1.5, 5, and 24 h). (**B**) Cytotoxicity of exosomes incubated for the indicated time points with tumor cells of different histotypes of both hematological (Jurkat, K562, and DAUDI) and solid (SKBR3 and 501mel) origin. (**C**) Lytic activity of exosomes toward both autologous PBMC and PHA-activated PBMC, isolated from healthy donors. All the cytolytic assays data (percentage of specific lysis ± SD) are representative of three independent series of experiments performed in triplicate. (**D**) CLSM analysis of Jurkat or K562 cell death after incubation with LAKEXO for 5 h and stained with supravital PI (red) dose. Nuclei were stained with DAPI (blue). The "spotted" nucleus represents apoptotic cells (whole arrow), whereas the diffused red staining represents necrotic cells (head arrow). (**E**) Histograms of the PI supravital uptake (Ref. 30) of a representative experiment in which Jurkat cells were incubated with LAKEXO at indicated time points, in absence (□) or presence (■) of neutralizing mAb anti-Fas ZB4 (100 ng/ml). Data are representative of two to three independent experiments.

cells appeared to be resistant to the cytotoxic effect of NK-derived exosomes.

To preliminary explore the predominant cell death pathway induced by NK cell-derived exosomes, we used cellular targets undergoing cell death through either FasL-mediated apoptosis (Jurkat cells) or necrosis (K562 cells), analyzing the results by a method based on PI uptake, allowing to distinguish simultaneously apoptotic, necrotic, and living cells (30). CLSM analyses (Fig. 4D) showed the contemporary occurrence of apoptosis and necrosis in both cell targets. Preincubation of Jurkat cells with the neutralizing anti-Fas mAb ZB4 did not substantially modify the level of cell death induced by LAKEXO (Fig. 4E, Table I), suggesting that the exosome-mediated cytotoxicity was mostly due to perforin.

NK-derived exosomes interaction with target cells

Exosomes may undergo uptake by tumor cells through a fusion-mediated mechanism (17). Therefore, the following set of experiments was dedicated to investigate the occurrence of NKEXO uptake by target cells by CLSM analyses. Fig. 5A (and a magnified image in Fig. 5B) showed that LAKEXO, labeled with NHS-Rhodamine dye (red), were detected, after 5 h of incubation, inside the Jurkat cells (labeled with PKH67 dye, green). No evidence of LAKEXO uptake was obtained when we used resting PBMC as target cells (Fig. 5C).

Detection and cytotoxic activity of plasma-derived exosomes

Exosomes circulate in the human body of both healthy individuals and cancer patients (21, 27). So far, our data have shown that NK cells release exosomes that together with expressing markers of their cellular source (i.e., NKG2D, CD56, NKp30, NKp46, and NKp44 proteins) are able to exert an NK activity. However, we did not have the evidence that NK-derived exosomes were detectable in the plasma of human healthy individuals. We thus purified exosomes from the plasma of 11 healthy donors, as previously described (21, 27), testing the presence of both exosome- and NK-cell markers in purified preparations. Flow cytometry analysis of exosomes–bead complexes showed that plasmatic exosomes from healthy individuals expressed significant levels of CD56, NKp46, and NKG2D, whereas they were almost negative for NKp30, NKp44, CD3, CD4, and CD8 (Fig. 6A).

Plasmatic exosomes were further purified in a continuous sucrose gradient, and analyzed for perforin and Rab5B proteins expression. As shown in Fig. 6B, perforin and Rab5B were preferentially contained in the same fractions ranging from 1.11 to 1.23 g ml^{-1} density. To define the cellular origin of the perforin-positive plasma exosomes, we submitted the human plasma to further purification by incubating the whole plasma exosomes with anti–CD56-coated latex beads as compared with beads coated with an irrelevant anti-Flag Ab or directly to beads, and fractions were next analyzed by Western blotting. The results showed that

Table I. PI supravital uptake of Jurkat cells incubated with NKEXO

	Time of Coculture					
	1.5 h		5 h		24 h	
mAb ZB4	−	+	−	+	−	+
% apoptosis	28	27	16	13	11	9
% necrosis	8	9	8	6	3	3

Representative experiment of PI supravital uptake in which Jurkat cells were incubated with NKEXO at indicated time points (time of coculture), in absence (−) or presence (+) of neutralizing mAb anti-Fas ZB4 (100 ng/ml). The values indicates the relative percentages of apoptosis and necrosis derived from the PI supravital histograms (see Fig. 4E).

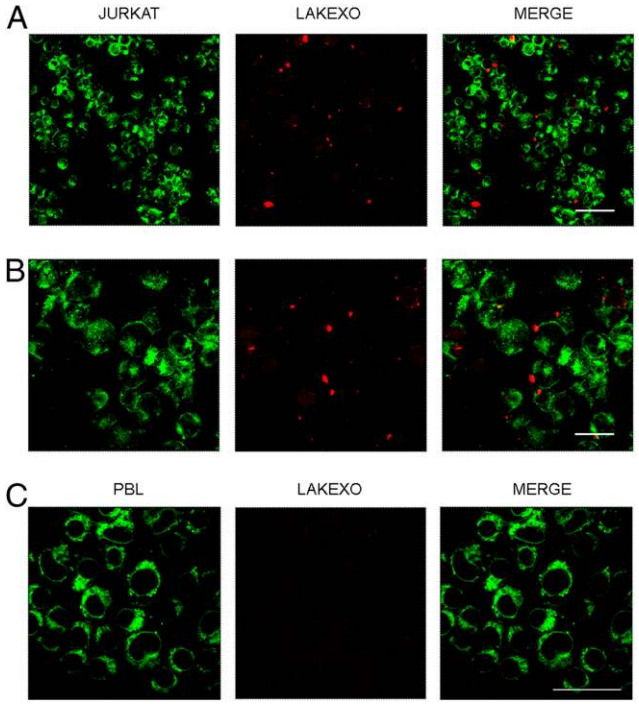

FIGURE 5. NK-derived exosomes interaction with target cells. (**A**) An optical central section obtained by confocal laser scanning analysis of Jurkat cells stained with PKH67 dye (green) and LAKEXO labeled with NHS-Rhodamine dye (red), coincubated for 5 h. Scale bar, 50 μm. (**B**) A magnified image (×3) of (**A**). Scale bar, 15 μm. (**C**) PBMC stained with PHK67 dye (green) and NKEXO labeled with NHS-Rhodamine dye, coincubated for 5 h. Scale bar, 24 μm. These results were confirmed by three independent series of experiments.

the $CD56^+$ latex bead-bound exosomes were enriched in a 75-kDa band corresponding to perforin, which was undetectable in Flag Ab latex bead- and was less detectable in directly bound exosomes (Fig. 6C), suggesting that only a subpopulation of NK exosomes was detectable in plasma of human healthy donors.

We finally investigated potential bioactivity of plasmatic exosomes obtained by differential centrifugation (26). To this aim, we cocultured whole plasma exosomes with target cells (Jurkat, K562, and DAUDI cells), evaluating exosome-induced cytotoxicity at different time points (1.5, 5, and 24 h). Notably, plasmatic exosomes displayed cytolytic activity against different human tumor target cells and activated PBMC as well (Fig. 6D, 6E) while at a lower level as compared with exosomes purified from NK cell culture supernatants.

Discussion

In this study, we show that NK cells secrete exosomes in a constitutive way and, differently to B and T cells, independently from their activation level (12, 32) and with a great variability, both in terms of exosomes amount and of NK-related protein expression, among the individual healthy donors analyzed.

CD56 (neuronal-cell adhesion molecule) is constitutively expressed by both NK- and LAK-derived exosomes. The CD56 expression may be involved in facilitating adhesion of exosomes to target cells. In fact, expression of adhesion receptors, such as ICAM-1, on dendritic cell-derived exosomes has been reported to be essential in facilitating interaction between APCs and T cells in promoting a potent immune response (33). Together with CD56, NK exosomes express detectable amounts of the activating receptor NKG2D, whereas natural cytotoxicity receptors (NCRs),

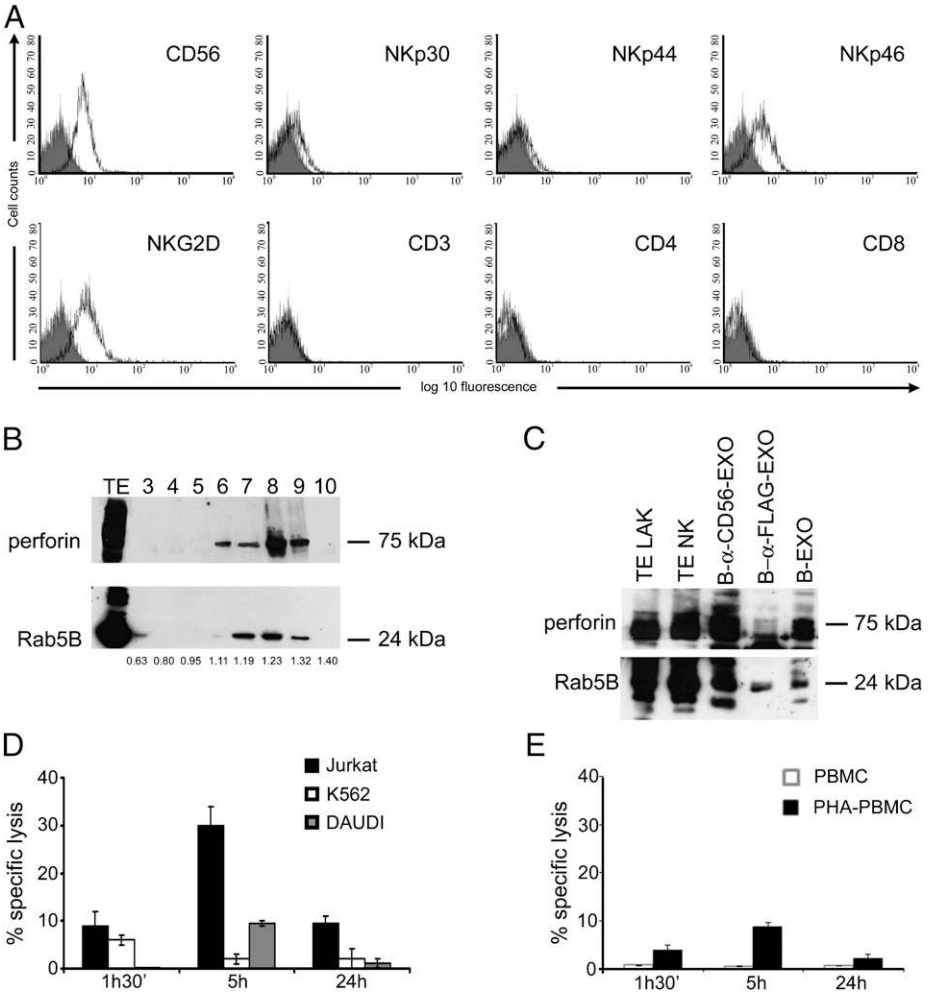

FIGURE 6. Detection of NKEXO in human plasma and cytolitic activity of plasmatic exosomes of healthy donors. (**A**) Flow cytometry analyses of plasma-derived exosomes linked to latex beads (4-μm diameter) and stained with the indicated primary Abs and then with Alexa Fluor 488-conjugated secondary Abs. The histograms shown in gray correspond to the isotype controls of the respective Abs, whereas the white histograms indicate the positive fluorescence. Representative examples of at least five independent experiments were reported. (**B**) Sucrose gradient fractions of plasma-derived exosomes blotted for perforin and Rab5B molecules. TE, total cell protein extract. (**C**) Western blot analysis of plasma-derived exosomes linked to latex beads (B-EXO) or preincubated with anti-CD56 (B-α-CD56-EXO) or irrelevant anti-FLAG (B-α-FLAG-EXO) Abs and blotted with anti-perforin and anti-Rab5B Abs. TE LAK and TE NK, LAK and NK cells total protein extracts, respectively. Data are representative of two experiments. (**D** and **E**) Cytolytic activity of plasma exosomes incubated for the indicated time points with tumor cells of hematological histotype origin (Jurkat, K562, and DAUDI) (D), and with normal resting or activated cells (PBMC and PHA-PBMC cells) (E). The data (percentage of specific lysis ± SD) are representative of three independent series of experiments performed in triplicate.

the other NK receptors directly involved in natural cytotoxicity (NKp30, NKp46, and NKp44), are less expressed. These data are consistent with the finding that a role of NKG2D is better appreciated in NK-mediated tumor cell killing exerted by NK cells expressing low NCRs surface densities (34, 35). It is also conceivable that the high levels of NKG2D on NK-derived exosomes may be involved in the NK-mediated surveillance of primary tumors. In fact, the role of NKG2D is now emerging in the control of tumorigenesis (36), supported also by the upregulation of NKG2D ligands in tumor cells (37).

We also showed that FasL molecules are expressed in a similar amount on both NK- and LAK-derived exosomes. Biochemical analyses in resting and activated NK exosomes demonstrated the presence of the membrane isoform of FasL (40 kDa) and that of a band at a higher molecular mass (~50 kDa), probably as a result of different regulatory posttranscriptional modifications for an efficient targeting of FasL to the various cellular compartments (38). Intriguingly, these analyses revealed also the presence of the soluble FasL isoform (sFasL), which is known to be a major player in the activation-induced death of T lymphoma-derived cells (39). We showed that NKEXO and LAKEXO exert cytotoxic activity against tumors of different histologies but also against activated PBMC derived from healthy donors, being ineffective against resting cells.

It is worth noting that FasL expressed by NK cells contributes to the suppression of tumor growth in vivo (40), whereas the expression of this death ligand by activated T lymphocytes and secreted microvesicles assumes a key role in regulating peripheral tolerance and lymphocyte homeostasis (19). We previously reported that human melanoma and colorectal cancer-derived exosomes express the proapoptotic molecules FasL and/or TRAIL, involved in induction of T cell death (18, 20), thus contributing to tumor immune escape. In contrast, FasL may be stored in specialized secretory lysosomal-like particles delivered to the cell surface through a controlled polarized degranulation (5). Thus, our data suggest that FasL-positive NK-derived exosomes, differently to the secretory lysosomes, might operate in a paracrine way, within tissues, and at distance getting to different target organs by circulating into the blood flow. It is conceivable that tumors do not express a functional Fas receptor, being mostly not susceptible to Fas triggering by FasL (41). Our results suggest a potential role of FasL expressed on NK-derived exosomes in regulating lymphocytes homeostasis. At the same time, we cannot exclude a possible cytolytic role of the soluble isoform of FasL identified in NK-derived exosomes. In this paper, we demonstrate that NK-derived exosomes undergo uptake by target cells. This may suggest a further hypothesis on a new exosome-mediated cell death mechanism, through which sFasL contained into NK-derived exosomes, may induce Fas-mediated cell death following uptake by target cells and interaction with some internal structures. Of course this should represent an entirely not known apoptotic pathway, deserving an entirely new and dedicated study to be better understood. Moreover, our study also shows that NKEXO and LAKEXO contain perforin, usually stored in the lytic granules of CTLs and NK cells (4). In sum, the data of this study suggest that NKEXO could trigger target cell death by two distinct mechanisms: 1) a classical ligand/receptor

interaction between mFasL of NKEXO and Fas on the target cell membrane; or 2) an unconventional cytotoxicity triggered by the uptaken exosomes inside the target cells and possibly mediated by the internal release of effectors molecules (i.e., perforin).

Taken together with the evidence that NK-released exosomes may exert a cytotoxic activity against target cells, we have also shown that exosomes expressing NK cell markers circulate in the plasma of healthy donors, they are fully functional and able to induce cytotoxicity against target cells, but they are completely ineffective against resting normal cells. Obviously, the amount of NK-derived exosomes purified from plasma of a single donor was much lower as compared with the amount of exosomes purified from NK cell culture supernatants. However, a portion of plasmatic exosomes expressed both perforin and CD56 molecules. Perforin-containing plasmatic exosomes were exclusively associated with NK markers, being $CD8^+$ T cell markers virtually undetectable. This result is consistent with a recent study showing that perforin is highly expressed in resting NK cells but not in resting $CD8^+$ T lymphocytes (42).

It is worth noting that perforin molecules are highly conserved in divergent species, thus strengthening the ancestral role ascribed to perforin in the immune responses of heterogeneous living organisms (43). Such a high level of conservation of perforin over at least 300 million years of evolution and, contrarily to granzymes, the lack of isoforms suggest that perforin might have some biological properties with some important universal features (43). In the past two decades a growing body of evidence is supporting a key role of perforin in the control of tumor initiation, growth, and spreading. As an example, perforin-deficient mice are profoundly immunocompromised and more prone to develop spontaneous tumors (44). The $perforin^+/CD56^+$ exosomes found among plasma exosomes expressed high levels of NKp46, a receptor directly involved in the binding of the viral hemagglutinin protein (45), and NKG2D molecules, involved in the control of tumorigenesis (36), thus strengthening a possible role of NK-derived exosomes in both antiviral and natural antitumor responses.

Among the numerous mechanisms responsible for the failure of immunotherapy, the role of the acidic microenvironment within solid tumors has emerged (46). This seems the case of human NK and LAK cells as well, whose cytotoxicity against a variety of tumors was inhibited by an acidic extracellular pH, thus inhibiting both the release of perforin/granzyme-containing granules and the Fas/FasL interaction (47). Recently, we have demonstrated that the acidic tumor microenvironment facilitates exosomes uptake by tumor cells (17). Therefore, future antitumor strategies might be based on NK-derived exosomes, instead of the whole cell, thus possibly overcoming the incapability of NK cells to explain their cytolytic activity.

In the light of our results, exosomes may represent an ideal example of biomimetism, that should be taken into careful consideration for the future approaches in the nanomedicine field. The killer exosomes may well represent a clear example of circulating nanovectors, delivering cytotoxic molecules, potentially highly effective against either infectious agents or tumor cells, exerting a key role in the control of immune response as well.

Disclosures

The authors have no financial conflicts of interest.

References

1. Griffiths, G. M. 1996. Secretory lysosomes - a special mechanism of regulated secretion in haemopoietic cells. *Trends Cell Biol.* 6: 329–332.
2. Blott, E. J., and G. M. Griffiths. 2002. Secretory lysosomes. *Nat. Rev. Mol. Cell Biol.* 3: 122–131.
3. Lowin, B., M. C. Peitsch, and J. Tschopp. 1995. Perforin and granzymes: crucial effector molecules in cytolytic T lymphocyte and natural killer cell-mediated cytotoxicity. *Curr. Top. Microbiol. Immunol.* 198: 1–24.
4. Lettau, M., H. Schmidt, D. Kabelitz, and O. Janssen. 2007. Secretory lysosomes and their cargo in T and NK cells. *Immunol. Lett.* 108: 10–19.
5. Bossi, G., and G. M. Griffiths. 1999. Degranulation plays an essential part in regulating cell surface expression of Fas ligand in T cells and natural killer cells. *Nat. Med.* 5: 90–96.
6. Peters, P. J., H. J. Geuze, H. A. van der Donk, and J. Borst. 1990. A new model for lethal hit delivery by cytotoxic T lymphocytes. *Immunol. Today* 11: 28–32.
7. Théry, C., M. Ostrowski, and E. Segura. 2009. Membrane vesicles as conveyors of immune responses. *Nat. Rev. Immunol.* 9: 581–593.
8. Horstman, L. L., W. Jy, A. Minagar, C. J. Bidot, J. J. Jimenez, J. S. Alexander, and Y. S. Ahn. 2007. Cell-derived microparticles and exosomes in neuroinflammatory disorders. *Int. Rev. Neurobiol.* 79: 227–268.
9. Onlamoon, N., K. Pattanapanyasat, and A. A. Ansari. 2005. Human and nonhuman primate lentiviral infection and autoimmunity. *Ann. N. Y. Acad. Sci.* 1050: 397–409.
10. Théry, C., L. Zitvogel, and S. Amigorena. 2002. Exosomes: composition, biogenesis and function. *Nat. Rev. Immunol.* 2: 569–579.
11. Schorey, J. S., and S. Bhatnagar. 2008. Exosome function: from tumor immunology to pathogen biology. *Traffic* 9: 871–881.
12. Raposo, G., H. W. Nijman, W. Stoorvogel, R. Liejendekker, C. V. Harding, C. J. Melief, and H. J. Geuze. 1996. B lymphocytes secrete antigen-presenting vesicles. *J. Exp. Med.* 183: 1161–1172.
13. Denzer, K., M. J. Kleijmeer, H. F. Heijnen, W. Stoorvogel, and H. J. Geuze. 2000. Exosome: from internal vesicle of the multivesicular body to intercellular signaling device. *J. Cell Sci.* 113: 3365–3374.
14. Valadi, H., K. Ekström, A. Bossios, M. Sjöstrand, J. J. Lee, and J. O. Lötvall. 2007. Exosome-mediated transfer of mRNAs and microRNAs is a novel mechanism of genetic exchange between cells. *Nat. Cell Biol.* 9: 654–659.
15. Tumne, A., V. S. Prasad, Y. Chen, D. B. Stolz, K. Saha, D. M. Ratner, M. Ding, S. C. Watkins, and P. Gupta. 2009. Noncytotoxic suppression of human immunodeficiency virus type 1 transcription by exosomes secreted from $CD8^+$ T cells. *J. Virol.* 83: 4354–4364.
16. Iero, M., R. Valenti, V. Huber, P. Filipazzi, G. Parmiani, S. Fais, and L. Rivoltini. 2008. Tumour-released exosomes and their implications in cancer immunity. *Cell Death Differ.* 15: 80–88.
17. Parolini, I., C. Federici, C. Raggi, L. Lugini, S. Palleschi, A. De Milito, C. Coscia, E. Iessi, M. Logozzi, A. Molinari, et al. 2009. Microenvironmental pH is a key factor for exosome traffic in tumor cells. *J. Biol. Chem.* 284: 34211–34222.
18. Andreola, G., L. Rivoltini, C. Castelli, V. Huber, P. Perego, P. Deho, P. Squarcina, P. Accornero, F. Lozupone, L. Lugini, et al. 2002. Induction of lymphocyte apoptosis by tumor cell secretion of FasL-bearing microvesicles. *J. Exp. Med.* 195: 1303–1316.
19. Martínez-Lorenzo, M. J., A. Anel, S. Gamen, I. Monle n, P. Lasierra, L. Larrad, A. Piñeiro, M. A. Alava, and J. Naval. 1999. Activated human T cells release bioactive Fas ligand and APO2 ligand in microvesicles. *J. Immunol.* 163: 1274–1281.
20. Huber, V., S. Fais, M. Iero, L. Lugini, P. Canese, P. Squarcina, A. Zaccheddu, M. Colone, G. Arancia, M. Gentile, et al. 2005. Human colorectal cancer cells induce T-cell death through release of proapoptotic microvesicles: role in immune escape. *Gastroenterology* 128: 1796–1804.
21. Logozzi, M., A. De Milito, L. Lugini, M. Borghi, L. Calabrò, M. Spada, M. Perdicchio, M. L. Marino, C. Federici, E. Iessi, et al. 2009. High levels of exosomes expressing CD63 and caveolin-1 in plasma of melanoma patients. *PLoS One* 4: e5219.
22. Delcayre, A., H. Shu, and J. B. Le Pecq. 2005. Dendritic cell-derived exosomes in cancer immunotherapy: exploiting nature's antigen delivery pathway. *Expert Rev. Anticancer Ther.* 5: 537–547.
23. Le Pecq, J. B. 2005. Dexosomes as a therapeutic cancer vaccine: from bench to bedside. *Blood Cells Mol. Dis.* 35: 129–135.
24. Perussia, B., C. Ramoni, I. Anegon, M. C. Cuturi, J. Faust, and G. Trinchieri. 1987. Preferential proliferation of natural killer cells among peripheral blood mononuclear cells cocultured with B lymphoblastoid cell lines. *Nat. Immun. Cell Growth Regul.* 6: 171–188.
25. Kawakami, Y., S. Eliyahu, C. H. Delgado, P. F. Robbins, L. Rivoltini, S. L. Topalian, T. Miki, and S. A. Rosenberg. 1994. Cloning of the gene coding for a shared human melanoma antigen recognized by autologous T cells infiltrating into tumor. *Proc. Natl. Acad. Sci. USA* 91: 3515–3519.
26. Théry, C., S. Amigorena, G. Raposo, and A. Clayton. 2006. Isolation and characterization of exosomes from cell culture supernatants and biological fluids. *Curr. Protoc. Cell Biol.* Unit 3.22.1-3.22.29.
27. Caby, M. P., D. Lankar, C. Vincendeau-Scherrer, G. Raposo, and C. Bonnerot. 2005. Exosomal-like vesicles are present in human blood plasma. *Int. Immunol.* 17: 879–887.
28. Derby, E., V. Reddy, W. Kopp, E. Nelson, M. Baseler, T. Sayers, and A. Malyguine. 2001. Three-color flow cytometric assay for the study of the mechanisms of cell-mediated cytotoxicity. *Immunol. Lett.* 78: 35–39.
29. Cecchetti, S., F. Spadaro, L. Lugini, F. Podo, and C. Ramoni. 2007. Functional role of phosphatidylcholine-specific phospholipase C in regulating CD16 membrane expression in natural killer cells. *Eur. J. Immunol.* 37: 2912–2922.
30. Zamai, L., E. Falcieri, G. Marhefka, and M. Vitale. 1996. Supravital exposure to propidium iodide identifies apoptotic cells in the absence of nucleosomal DNA fragmentation. *Cytometry* 23: 303-311.
31. Hirota, Y., T. Kuronita, H. Fujita, and Y. Tanaka. 2007. A role for Rab5 activity in the biogenesis of endosomal and lysosomal compartments. *Biochem. Biophys. Res. Commun.* 364: 40–47.

32. Peters, P. J., H. J. Geuze, H. A. Van der Donk, J. W. Slot, J. M. Griffith, N. J. Stam, H. C. Clevers, and J. Borst. 1989. Molecules relevant for T cell-target cell interaction are present in cytolytic granules of human T lymphocytes. *Eur. J. Immunol.* 19: 1469–1475.
33. Segura, E., C. Nicco, B. Lombard, P. Véron, G. Raposo, F. Batteux, S. Amigorena, and C. Théry. 2005. ICAM-1 on exosomes from mature dendritic cells is critical for efficient naive T-cell priming. *Blood* 106: 216–223.
34. Pende, D., C. Cantoni, P. Rivera, M. Vitale, R. Castriconi, S. Marcenaro, M. Nanni, R. Biassoni, C. Bottino, A. Moretta, and L. Moretta. 2001. Role of NKG2D in tumor cell lysis mediated by human NK cells: cooperation with natural cytotoxicity receptors and capability of recognizing tumors of non-epithelial origin. *Eur. J. Immunol.* 31: 1076–1086.
35. Sivori, S., D. Pende, C. Bottino, E. Marcenaro, A. Pessino, R. Biassoni, L. Moretta, and A. Moretta. 1999. NKp46 is the major triggering receptor involved in the natural cytotoxicity of fresh or cultured human NK cells. Correlation between surface density of NKp46 and natural cytotoxicity against autologous, allogeneic or xenogeneic target cells. *Eur. J. Immunol.* 29: 1656–1666.
36. Guerra, N., Y. X. Tan, N. T. Joncker, A. Choy, F. Gallardo, N. Xiong, S. Knoblaugh, D. Cado, N. M. Greenberg, and D. H. Raulet. 2008. NKG2D-deficient mice are defective in tumor surveillance in models of spontaneous malignancy. *Immunity* 28: 571–580.
37. Bauer, S., V. Groh, J. Wu, A. Steinle, J. H. Phillips, L. L. Lanier, and T. Spies. 1999. Activation of NK cells and T cells by NKG2D, a receptor for stress-inducible MICA. *Science* 285: 727–729.
38. Zuccato, E., E. J. Blott, O. Holt, S. Sigismund, M. Shaw, G. Bossi, and G. M. Griffiths. 2007. Sorting of Fas ligand to secretory lysosomes is regulated by mono-ubiquitylation and phosphorylation. *J. Cell Sci.* 120: 191–199.
39. Martínez-Lorenzo, M. J., M. A. Alava, A. Anel, A. Piñeiro, and J. Naval. 1996. Release of preformed Fas ligand in soluble form is the major factor for activation-induced death of Jurkat T cells. *Immunology* 89: 511–517.
40. Bradley, M., A. Zeytun, A. Rafi-Janajreh, P. S. Nagarkatti, and M. Nagarkatti. 1998. Role of spontaneous and interleukin-2-induced natural killer cell activity in the cytotoxicity and rejection of Fas^+ and Fas^- tumor cells. *Blood* 92: 4248–4255.
41. Houston, A., and J. O'Connell. 2004. The Fas signalling pathway and its role in the pathogenesis of cancer. *Curr. Opin. Pharmacol.* 4: 321–326.
42. Obata-Onai, A., S. Hashimoto, N. Onai, M. Kurachi, S. Nagai, K. Shizuno, T. Nagahata, and K. Matsushima. 2002. Comprehensive gene expression analysis of human NK cells and $CD8^+$ T lymphocytes. *Int. Immunol.* 14: 1085–1098.
43. Hwang, J. Y., T. Ohira, I. Hirono, and T. Aoki. 2004. A pore-forming protein, perforin, from a non-mammalian organism, Japanese flounder, *Paralichthys olivaceus*. *Immunogenetics* 56: 360–367.
44. Smyth, M. J., K. Y. Thia, S. E. Street, D. MacGregor, D. I. Godfrey, and J. A. Trapani. 2000. Perforin-mediated cytotoxicity is critical for surveillance of spontaneous lymphoma. *J. Exp. Med.* 192: 755–760.
45. Mandelboim, O., N. Lieberman, M. Lev, L. Paul, T. I. Arnon, Y. Bushkin, D. M. Davis, J. L. Strominger, J. W. Yewdell, and A. Porgador. 2001. Recognition of haemagglutinins on virus-infected cells by NKp46 activates lysis by human NK cells. *Nature* 409: 1055–1060.
46. Helmlinger, G., F. Yuan, M. Dellian, and R. K. Jain. 1997. Interstitial pH and pO2 gradients in solid tumors in vivo: high-resolution measurements reveal a lack of correlation. *Nat. Med.* 3: 177–182.
47. Fischer, B., B. Müller, K. G. Fischer, N. Baur, and W. Kreutz. 2000. Acidic pH inhibits non-MHC-restricted killer cell functions. *Clin. Immunol.* 96: 252–263.